Sulfide alters microbial functional potential in a methane and nitrogen cycling biofilm reactor

Jeseth Delgado Vela [iD],[1] Laura A. Bristow [iD],[2] Hannah K. Marchant [iD],[3] Nancy G. Love [iD][4] and Gregory J. Dick [iD][5*]

[1]*Department of Civil and Environmental Engineering, Howard University, Washington, DC.*

[2]*Department of Biology, University of Southern Denmark, Odense, Denmark.*

[3]*Max Planck Institute for Marine Microbiology, Bremen, Germany.*

[4]*Department of Civil and Environmental Engineering, University of Michigan, Ann Arbor, MI.*

[5]*Department of Earth and Environmental Sciences, University of Michigan, Ann Arbor, MI.*

Summary

Cross-feeding of metabolites between coexisting cells leads to complex and interconnected elemental cycling and microbial interactions. These relationships influence overall community function and can be altered by changes in substrate availability. Here, we used isotopic rate measurements and metagenomic sequencing to study how cross-feeding relationships changed in response to stepwise increases of sulfide concentrations in a membrane-aerated biofilm reactor that was fed with methane and ammonium. Results showed that sulfide: (i) decreased nitrite oxidation rates but increased ammonia oxidation rates; (ii) changed the denitrifying community and increased nitrous oxide production; and (iii) induced dissimilatory nitrite reduction to ammonium (DNRA). We infer that inhibition of nitrite oxidation resulted in higher nitrite availability for DNRA, anammox, and nitrite-dependent anaerobic methane oxidation. In other words, sulfide likely disrupted microbial cross-feeding between AOB and NOB and induced cross-feeding between AOB and nitrite reducing organisms. Furthermore, these cross-feeding relationships were spatially distributed between biofilm and planktonic phases of the reactor.

These results indicate that using sulfide as an electron donor will promote N_2O and ammonium production, which is generally not desirable in engineered systems.

Introduction

Although essential to cellular life, nitrogen can contaminate natural water bodies and contribute to global warming. Microbial processes control the nitrogen cycle; hence, human management of microbial activity can help mitigate environmental pollution. Understanding coupled biogeochemical cycling of nitrogen, sulfur, and carbon is complex due to the metabolic flexibility of the bacteria that cycle these substrates. For instance, marine nitrite-oxidizing bacteria have been shown to oxidize sulfide (Füssel *et al*., 2017), anammox bacteria can oxidize organic matter (Kartal *et al*., 2007), and sulfate-reducing bacteria can also denitrify (Thorup and Schramm, 2017). Due to this metabolic flexibility, taxonomic markers such as the 16S rRNA gene are insufficient to determine the key players in the sulfur, nitrogen, and carbon cycles. Indeed, new molecular and cultivation techniques (e.g. Raman-activated cell sorting, high throughput sequencing technology) have spurred rapid discovery in this area (Kuypers *et al*., 2018). In addition to metabolic flexibility, microbial community function is affected by metabolic interactions between different cells of different taxa. Microbial cross-feeding relationships, through which members of one taxa consume the reaction products from another taxonomic group, also affect elemental biogeochemical cycling (Seth and Taga, 2014; D'Souza *et al*., 2018; Marchant *et al*., 2018). High-resolution methods are needed to resolve these microbial interactions because they can be cryptic yet are important in both environmental (Canfield *et al*., 2010) and engineered systems (Delgado Vela *et al*., 2015b; Arshad *et al*., 2017).

Few laboratory-based bioreactor studies have evaluated the interactions between microbial cycling of methane, nitrogen, and sulfur in mixed redox environments. Cross feeding relationships are complex even in simple redox environments. For example, a recent study using a suspended culture anoxic bioreactor that simulated a

brackish sediment environment revealed the coexistence and beneficial cross-feeding relationship between anammox, sulfide oxidizers, and denitrifying anaerobic methane oxidizers (Arshad *et al*., 2017). The presence of anammox in a system supplied with sulfide is somewhat surprising because sulfide is typically thought to inhibit anammox bacteria (Jin *et al*., 2013). However, this is consistent with previous evidence showing sulfide-based denitrifiers enable anammox by consuming the inhibitory sulfide and reducing nitrate produced by anammox to either nitrite (Russ *et al*., 2014; Rios-Del Toro and Cervantes, 2016; Russ *et al*., 2019) or ammonia (Jones *et al*., 2017). Bioreactor environments that have a mixed redox environment further promote additional cross-feeding relationships. The introduction of oxygen allows the growth of aerobic bacteria such as nitrifiers, methanotrophs, and sulfur oxidizers, enabling additional cross-feeding relationships. The abundance of coupled oxic and anoxic environments in natural (e.g. Reim *et al*., 2012; Bristow *et al*., 2016; Lüke *et al*., 2016) and engineered (e.g. Morgenroth *et al*., 1997; Pochana and Keller, 1999) environments highlights the need to understand how microbial interactions in these systems shape elemental cycling and how those interactions change under different substrate conditions.

Bioreactor systems are well-suited for understanding microbial interactions because oxic and anoxic environments can be precisely created and controlled. Controlled experiments that create distinct environments in lab-scale bioreactors can be used to develop and test hypotheses on the metabolic interactions that may occur between different microbial groups. A membrane-aerated biofilm reactor (MABR) uses oxygen-permeable membranes to produce a counter-current biofilm where the flux of dissolved oxygen (from the membrane) moves in the opposite direction to the flow of electron donor (from the bulk liquid) (Terada *et al*., 2007; Martin and Nerenberg, 2012). MABRs provide a stratified redox environment that is appropriate for studying nitrogen and sulfur cycling; specifically, they provide a way to observe both microbial population selection in concert with nitrogen and sulfur speciation. In addition, MABRs are energy efficient, and thus are increasingly being considered for full-scale wastewater treatment (Heffernan *et al*., 2017; Houweling *et al*., 2017; Peeters *et al*., 2017). We contend that understanding how microbes interact in MABRs can inform our understanding of both microbial cross-feeding and bioreactor design approaches that achieve effective nitrogen removal.

In this study, we operated a lab-scale MABR and applied metagenomic and isotope labeling techniques to evaluate interactions between microbial populations. Given that previous studies have conflicting results with respect to the impact of sulfide on anammox bacteria (e.g. Jin *et al*., 2013; Arshad *et al*., 2017; Jones *et al*., 2017; Russ *et al*., 2019) and the potential for sulfide inhibition of nitrification (e.g. Joye and Hollibaugh, 1995; Delgado Vela *et al*., 2018), we were particularly interested in how microbial interactions and nitrogen cycling changed as a result of sulfide. We evaluated how sulfide changes rates of nitrogen redox reactions over short-term batch experiments, and how sulfide shifts the microbial community functional potential over long-term, stepwise increases in sulfide concentration. During bioreactor operation with a feed containing dissolved methane, sulfide, and ammonia, simultaneous oxic and anoxic cycling of nitrogen, sulfur, and carbon occurred. We identified nitrite sinks that were stimulated as a result of sulfide addition such as anammox, denitrifying anaerobic methane oxidizers, denitrifying sulfur oxidizers, and dissimilatory nitrite reduction to ammonia (DNRA). The importance of microbial cross-feeding relationships in this study is underscored as differential sulfide inhibition of ammonia-oxidizing bacteria (AOB) and nitrite-oxidizing bacteria (NOB) could increase nitrite availability. Sulfur and nitrogen are abundant in both the natural environment and engineered systems. These findings can help us understand the interactions between sulfur and nitrogen cycling, which can be broadly applied to other mixed-redox environments.

Results and discussion

An MABR was operated for 562 days. During this time, sulfide concentrations were increased in a stepwise manner (Table S1, Fig. 1). The full performance data over the course of the 562 days are provided in Figs S2, S3, and Table S2. Increases in sulfide addition were associated with increasing ammonium concentrations, but relatively constant net nitrate production, indicating that there were shifts in nitrogen cycling. Biomass samples were taken approximately monthly and a subset was submitted for sequencing (dashed lines Fig. 1). Towards the end of the reactor operation, at which point the MABR had been supplied with sulfide at a concentration of 312.5 μmol/L (10 mg/L) for 27 days, stable isotope labeling experiments with ^{15}N substrates were used to evaluate the functional potential of the bioreactor with or without sulfide. These experiments were carried out in duplicate with sulfide (days 547–551) and without sulfide (days 557–562) (see details in Table S2). We aimed to add approximately 312.5 μmol/L HS$^-$ to reflect the MABR conditions; however, rapid sulfide oxidation likely occurred during filling the reactor with influent, which took 15–20 min. Therefore, we took samples for 'initial' sulfide concentrations after filling and when mixing had been initiated, at which point sulfide concentrations were between 27 and 71 μmol/L.
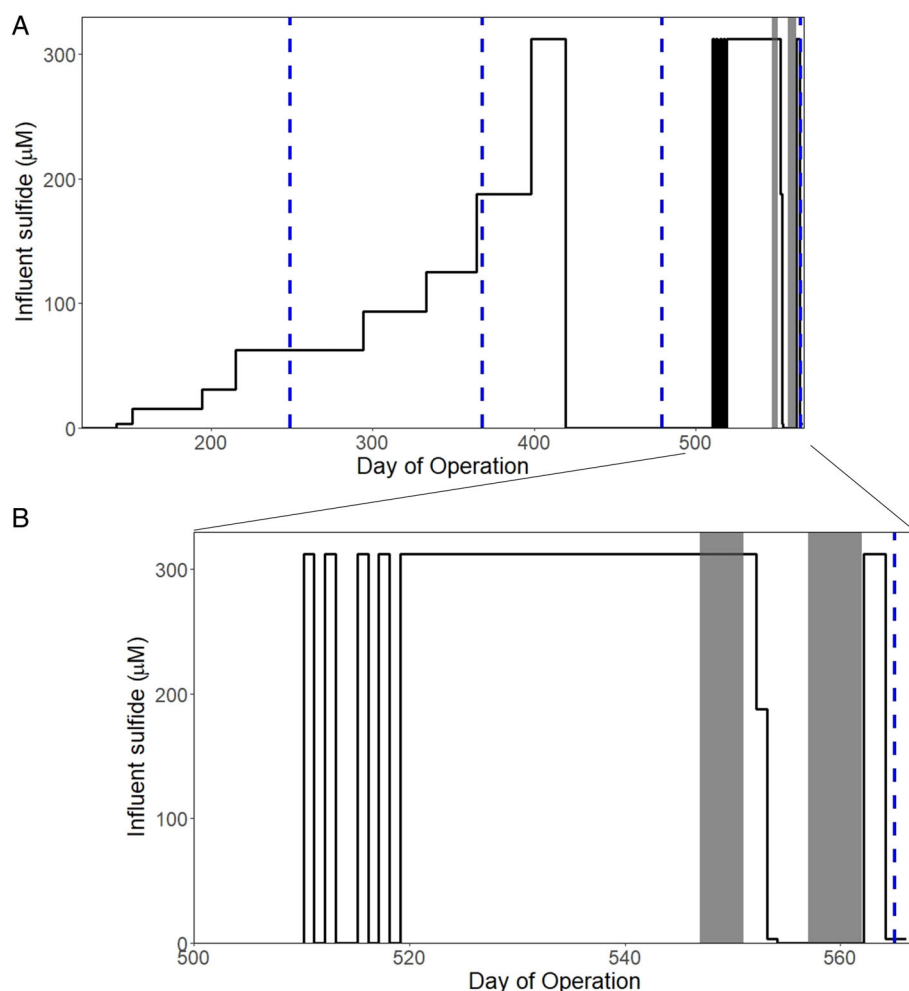
Sulfide addition decreased the relative abundance of nitrifier genes and nitrifying organisms, but only nitrite oxidation rates decreased in the presence of sulfide

Nitrification rates were determined using two different isotope labelling approaches, one with ^{15}N-NH_4^+ and ^{14}N-NO_2^- (ammonia oxidation, Fig. 2A) and one with ^{15}N-NO_2^- (nitrite oxidation, Fig. 2B). Ammonia oxidation rates were determined from the production of both ^{15}N-NO_2^- and ^{15}N-NO_3^- over time (Fig. 2C), which would also incorporate rates of complete ammonia oxidation to nitrate, as carried out by comammox bacteria. However, we believe this process is unlikely to have been substantial as almost no comammox ammonia oxidation genes were detected in the MABR (*amoB* Fig. 2D and *amoA* Fig. S5).

Ammonia oxidation rates were higher in the presence of sulfide (178 ± 5 μmol/L h) compared with zero sulfide experiments(86 ± 31 μmol/L h) (Fig. 2C). This indicates that ammonia oxidation was not inhibited by sulfide (concentrations ranging from 26.8 to 53.5 μM) in the rate experiments carried out on an MABR that had been previously fed sulfide. This contrasts with recent studies investigating the impact of sulfide addition in batch systems (Bejarano-Ortiz *et al*., 2015; Delgado Vela *et al*., 2018). However, these initial sulfide concentrations are lower than previously determined inhibition constants for AOB (298–388 μM) (Delgado Vela *et al*., 2018), therefore at higher initial sulfide concentrations, inhibition of AOB may still be an important process to consider. The lack of inhibition of ammonia oxidation by sulfide was unexpected, considering that ammonium concentrations were observed to increase over time during the long-term operation of the MABR (Fig. S3). These results were a first indication that ammonium concentrations may have been influenced by other nitrogen cycling processes (see section 'Sulfide increased potential for DNRA' below).

Nitrite oxidation rates were determined from the production of ^{15}N-NO_3^- after ^{15}N-NO_2^- addition, and in general were higher than ammonia oxidation rates. Furthermore, in contrast to ammonia oxidation, nitrite oxidation rates did not show a consistent trend with
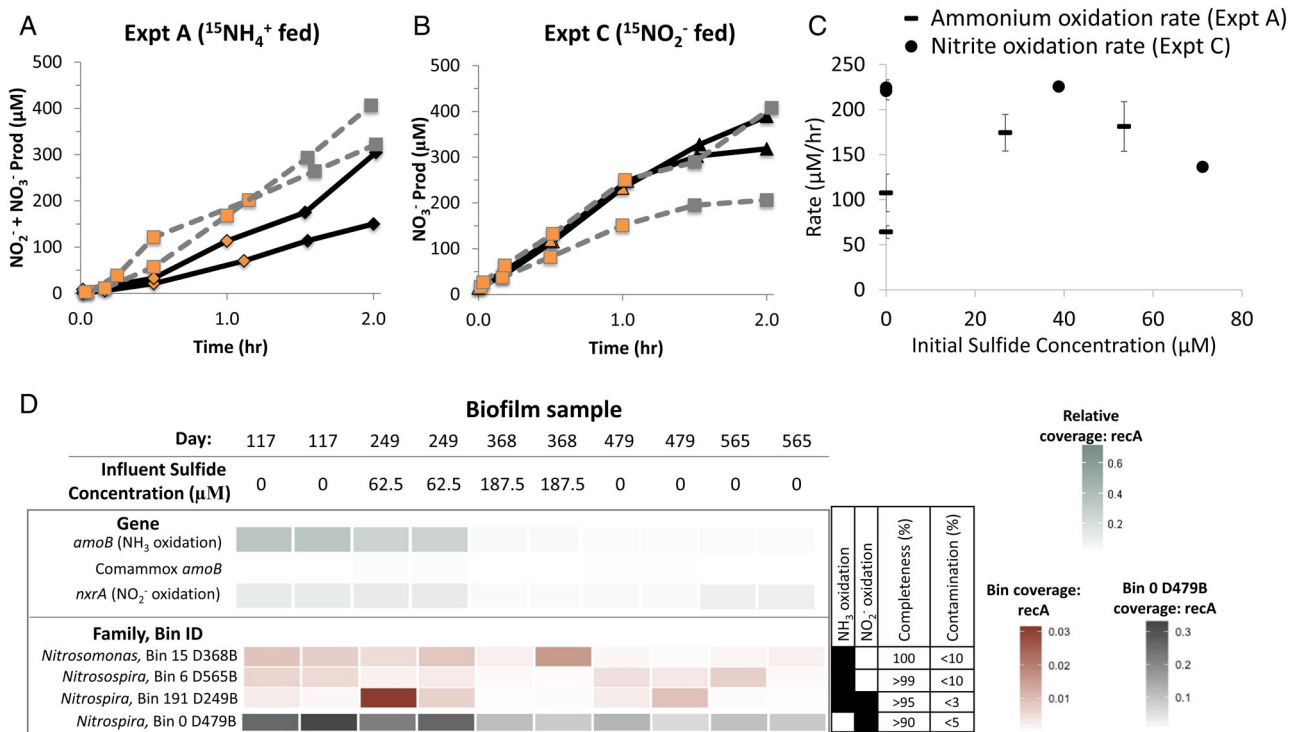
Fig 2. Nitrification trends with increasing sulfide.
A, B. Results from ^{15}N experiments which were conducted on days 547–551 and days 557–562. Dashed grey lines are sulfide amended; solid black lines are experiments without sulfide. Markers filled in orange indicate data points used for rate calculations.
C. Potential rates of ammonia oxidation and nitrite oxidation plotted against initial sulfide concentrations. Rates were inferred from the slopes of linear regression across the first hour of the experiment (data points used are shown by orange filled symbols, A and B). Error bars represent the standard error of the slope.
D. Relative coverage of nitrification gene markers decreases as sulfide increases, as do overall bin coverages. Coverage scale is based on the coverage of each gene normalized to total coverage of all bacterial *recA* genes.

increasing concentrations of sulfide. At the lower initial concentration of sulfide (40 μM), the nitrite oxidation rate did not differ from that with zero sulfide (226 and 223 ± 3 μmol/L h respectively). However, at 70 μM sulfide, nitrite oxidation rates dropped to 137 μmol/L h (Fig. 2C), suggesting NOB were inhibited by sulfide, consistent with previous studies (Erguder *et al*., 2008; Bejarano-Ortiz *et al*., 2015; Delgado Vela *et al*., 2018). These results are consistent with the inhibition index previously determined for a *Nitrospira*-dominated NOB population (81 ± 8 μM) (Delgado Vela *et al*., 2018). It is also worth noting that the 'initial' sulfide concentrations in Fig. 2C are from the sample taken as soon as mixing was initiated. However, rapid sulfide oxidation likely occurred during filling the reactor with influent, which took 15–20 min (prior to when mixing was initiated); therefore, these sulfide concentrations are probably underestimates of the true initial concentrations in the reactor. In addition, rate experiments occurred at the end of the stepwise increases in sulfide concentration so the nitrifying community may have already adapted to sulfide exposure. Similar to ammonia oxidation experiments, this result seemingly contrasts the long-term reactor data because

no nitrite accumulation was observed over the course of the experiment (Fig. S3). Of course, the long-term reactor data do not account for potential nitrite consumption that could be occurring. Despite this adaptation and uncertainty about sulfide concentration, there were clearly distinct effects of sulfide on ammonia oxidation and nitrite oxidation.

To explore how the nitrifying community adapted to sulfide, we evaluated the long-term effect of stepwise increases in sulfide on the microbial community present in different reactor compartments using metagenomic sequencing. Aerobic nitrifiers were confined to the biofilm portion of the reactor throughout the operating period (Figs S6 and 2D), likely because the planktonic portion was anoxic. As sulfide increased, the absolute and relative abundance of *nxrA* and *amoB* genes decreased (p_{ANOVA} = 0.01 for metagenomic reads, Figs 2D and S5), which indicates that nitrifying populations were decreasing. In addition, coverage of high-quality metagenome-assembled genomes (MAGs) from organisms carrying these genes (Fig. 2D) also decreased. Thus, the genetic data clearly show that the abundance of nitrifying bacteria decreased with long-term stepwise increases in sulfide.

These reductions in relative abundances are somewhat surprising given that rate experiments showed increased rates of ammonia oxidation in the presence of sulfide; however, this is consistent with the increased ammonium concentrations that were observed in the long-term reactor performance (Fig. S3).

To better understand the microbial community response to sulfide, we evaluated the metabolic potential of specific populations by analysing the gene content of MAGs. Both our nitrifier MAG coverage and qPCR data show that the relative and absolute abundances of *Nitrospira*-NOB were significantly higher than AOB (Figs 2A and S5). One potential explanation for this is that the reactor contained comammox bacteria, a *Nitrospira* that can oxidize ammonia to nitrate (Daims *et al*., 2015; van Kessel *et al*., 2015). We recovered one high-quality *Nitrospira* MAG from comammox bacteria (Bin 191 D249B, 96% complete, 3% contamination) most closely related to *Ca*. Nitrospira nitrificans (ANI of 80.6%, Fig. S8). However, coverage of this bin across reactor operation was very low, and qPCR confirmed that gene copies of comammox *amoA* were two orders of magnitude lower than copies of canonical AOB and *Nitrospira* (Supplementary Information, Fig. S5). In contrast, the other high-quality *Nitrospira* MAG (Bin 0 D479B, 91% complete, 4% contamination) was more abundant than the recovered AOB MAGs but did not contain genes for ammonia oxidation, indicating that it is incapable of comammox. Bin 0 D479B is most closely related to *Nitrospira* sp. defluvii, with an ANI of 78% (Fig. S8). This bin contains an *sqr* gene encoding for sulfide quinone reductase, a sulfide-oxidizing enzyme that is involved in energy conservation or sulfide detoxification (Luebke *et al*., 2014; Xia *et al*., 2017), suggesting that this *Nitrospira* population is tolerant of sulfide. *sqr* genes have been identified in *Nitrospira* sp. defluvii and other *Nitrospira* species (Lucker *et al*., 2010; Koch *et al*., 2015), and sulfide oxidation by NOB (*Nitrococcus*) has been reported (Füssel *et al*., 2017), but to our knowledge, there is no published evidence of sulfide oxidation by *Nitrospira*. Sulfide catabolism by *Nitrospira* could be a yet-uncovered mechanism that would explain the higher abundances of *Nitrospira* relative to AOB. Overall, the metagenomic data show that although relative abundances of nitrifying bacteria decreased with stepwise increases of sulfide, nitrifying population with a putative sulfide detoxification mechanism were present at higher relative abundances than other nitrifiers.

Sulfide did not affect nitrate reduction but did increase nitrous oxide production rates

We also evaluated the effect of sulfide on rates of nitrate reduction, nitrous oxide production, and abundances of denitrification genes (Fig. 3A–C). Short-term rate experiments carried out at the end of reactor operation showed that increasing sulfide concentrations did not significantly affect rates of nitrate reduction to nitrite (p_{ANOVA} = 0.18, Fig. 3D) but did increase rates of nitrous oxide (N_2O) production (Fig. 3A and C). It is unclear whether these changes in N_2O production are due to stimulation of nitric oxide reduction, inhibition of nitrous oxide reduction, or increased N_2O production associated with ammonia oxidation. Others have shown increased emissions of N_2O in the presence of sulfide in a variety of environments (Brunet and Garcia-Gil, 1996; Senga *et al*., 2006; Murphy *et al*., 2020), including activated sludge (Manconi *et al*., 2006; Tugstas and Pavlostathis, 2007). One proposed explanation is that sulfide inhibits nitrous oxide reductase (Sorensen *et al*., 1980). Given our data, we could not eliminate any of these potential explanations; however, we gained further insights into the pathways for denitrification and nitrous oxide production using metagenomic sequencing.

Changes in the relative abundance of genes related to denitrification over the long-term, stepwise increases in sulfide in different reactor sampling locations revealed a division of labor between physical compartments of the reactor (Fig. 3E). However, it should be noted that the planktonic growth was cleaned from the reactor monthly, given our initial intent to focus on the biofilm community. Planktonic biomass was not present until after sulfide was added to the influent, at which point genes associated with denitrification were abundant in the planktonic portion of the reactor, indicating that nitrate produced in the biofilm by nitrifiers was used by planktonic denitrifiers. Therefore, cross-feeding relationships occurred not only within the biofilm but also between the two reactor compartments. The high relative abundance of denitrification in the planktonic phase is consistent with other studies of nitrogen removal in MABRs (Downing and Nerenberg, 2008). Unlike previous studies, here metagenomic sequencing also provided insights into the abundances of genes encoding the different steps of denitrification. Over the long-term increases in sulfide concentration, the relative abundances of genes for N_2O reduction (*nosZ*) increased, not to the same extent as those for NO_2^- reduction (*nirK* and *nirS*). This suggests that the addition of sulfide decreased the relative capacity for N_2O reduction compared with N_2O production. The addition of the planktonic phase also increased nitrate reduction capacity compared with the biofilm and likely contributed to increased NO_2^- availability as well. This additional NO_2^- could have allowed for more available substrate for NOB, leading to a cryptic nitrite cycle that encouraged higher abundances of NOB relative to AOB. These results highlight that cross-feeding relationships related
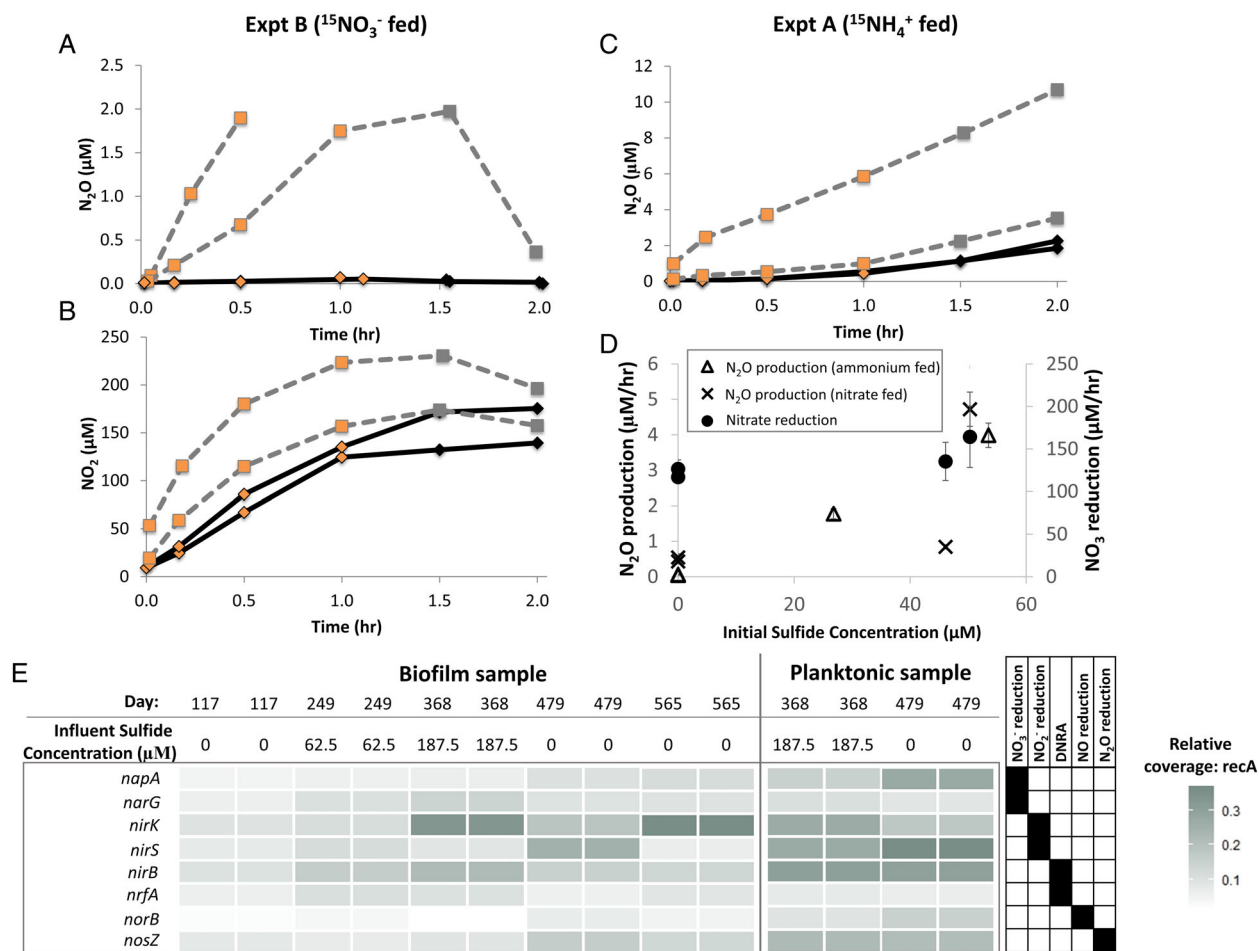
Fig 3. (A, B, C) Results from ^{15}N experiments which were conducted on days 547–551 and days 557–562. Dashed grey lines are sulfide amended; solid black lines are experiments without sulfide. Markers filled in orange indicate data points used for rate calculations.

D. Potential rates of nitrous oxide production (left scale) and nitrate reduction (right scale) plotted against initial sulfide concentrations. Rates were inferred from the slopes of linear regression across the first hour of the experiment (data points used are shown by orange filled symbols in A, B, and C), error bars represent the standard error of the slope.

E. Relative abundance of genes for key nitrogen reducing functions in the reactor. Coverage scale is based on the coverage of each gene normalized to total coverage of all bacterial *recA* genes. Nitrogen reduction gene markers are nitrate reductases (*napA* and *narG*), nitrite reductase (*nirK* and *nirS*), dissimilatory nitrite reduction to ammonia (DNRA, *nrfA,* and *nirB*), nitric oxide reductase (*norB*) and nitrous oxide reductase (*nosZ*).

to nitrate reduction were affected by sulfide in both planktonic and biofilm communities.

Given the wide range of electron donors present in the bioreactor and the diversity of possible denitrification-linked metabolisms (Delgado Vela *et al*., 2015b), we next evaluated the broader gene content of putative denitrifying MAGs in the two bioreactor compartments across the stepwise increases in sulfide (Fig. 4, MAGs with denitrifying genes and abundances greater than 5% in at least one sample). Among the more abundant microorganisms with the ability to reduce nitrogen in the biofilm at the end of the study were anammox (*Ca.* Brocadiaceae, Bin 154 D565S) and denitrifying anaerobic methane oxidizers (*Ca.* Methylomirabilis, Bin 23 D368S, Fig. 4), which were statistically correlated with influent

sulfide (p_{ANOVA} = 2.1E-5). It should be noted that despite the enrichment of this denitrifying anaerobic methane oxidizer over the course of the entire reactor operation, on average 81 ± 15% of the influent methane was oxidized (Table S2), and this did not change with increasing sulfide concentration. A Methylococcaceae bin is shown in Fig. 4 because it has the metabolic potential for partial denitrification and methane oxidation. Beck *et al*. (2013) similarly showed high abundances of a Methylococcaceae with a full denitrification pathway in the presence of nitrate in both aerobic and microaerobic sediment environments. However, it is unclear whether these nitrogen-reducing genes are used for assimilation or respiration (Osaka *et al*., 2008; Beck *et al*., 2013; Liu *et al*., 2014; Yu *et al*., 2017). One potential explanation is that as sulfide increased the
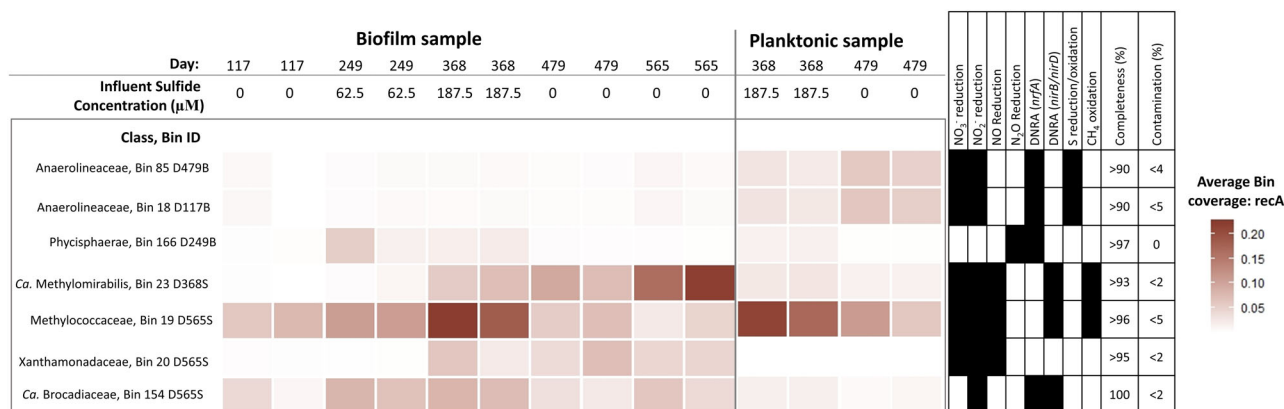
Fig 4. Genome bins containing genes for denitrification. Gene markers for nitrate reduction are *napA* or <u>*narG*</u>, nitrite reduction genes are *nirK* or *nirS*, nitric oxide reduction gene is *norB* , and nitrous oxide reduction gene is *nosZ*. S reduction/oxidation gene is either *soxB*, *soxA*, *dsrA*, *dsrB*, *aprA*, *sqr*, *fccA* or *fccB*, methane oxidation gene is either *pmoA* or *pmoB*. Metagenomic coverage is normalized to *recA* abundances. These bins were considered high-quality bins that had relative coverages greater than 5% in at least one sample.

Methylococcaceae outselected other aerobic methanotrophs because they are more adept to grow in microaerobic environments. However, given the genetic potential, this study shows that exploring methane-based denitrification by Methylococcaceae warrants further study. Others have also shown that oxidation of methane to methanol can support conventional heterotrophic denitrification (Modin *et al*., 2007), but we did not find any evidence for this mechanism in our study. Both anammox and *Ca*. Methylomirabilis use nitrite as their electron acceptor, thus the potential inhibition of nitrite oxidation by sulfide that was observed in the rate experiments could have provided increased substrate for anammox and denitrifying anaerobic methane oxidizers. Besides increased nitrite availability, a change in oxidation–reduction potential (ORP) induced by sulfide addition (Supplementary Information, Fig. S4) could stimulate the growth of anammox and denitrifying anaerobic methane-oxidizing organisms, which are both sensitive to oxygen (van de Graaf *et al*., 1996; Ettwig *et al*., 2010; Bristow *et al*., 2016; Guerrero-Cruz *et al*., 2018). These results indicate that it is possible to support anammox and denitrifying anaerobic methane oxidizers in a multi-redox MABR, and sulfide may promote this by inhibiting NOB and/or acting as a reducing agent.

The change in denitrifying taxa over the course of reactor operation offers another potential explanation for increased nitrous oxide production with increasing sulfide. As described earlier, sulfide led to a separation of denitrification labor between the planktonic and biofilm phase. The denitrifying potential that was in the planktonic biomass was sulfide-based denitrifiers, whereas the biofilm had a more diverse set of organisms that could reduce nitrate and nitrite (heterotrophs, anammox, and methane-based denitrifiers). When sulfide was present,

the sulfide-based denitrifiers in the planktonic phase were likely responsible for the reduction of nitrate and nitrite but did not have the metabolic capacity to complete the last two steps of denitrification (Fig. 4). Indeed, none of the bins in Fig. 4 that have the potential for dissimilatory sulfur metabolisms have nitrous oxide reduction potential via a nitrous oxide reductase. Therefore, nitrous oxide intermediates would need to diffuse into the biofilm to be completely reduced. It should be noted that nitrous oxide reduction potential in the planktonic phase did exist (Fig. 3E); however, this was associated with either MAGs that did not meet our quality thresholds or MAGs not shown in Fig. 4 because they were below 5% abundance in any samples (e.g. Bin 74 D368S). On the other hand, in the absence of sulfide, denitrification was likely confined to the biofilm and while intermediates may be produced and consumed by distinct organisms, these intermediates may not be measurable in the bulk liquid phase. These metagenomic results offer a potential alternative explanation for the observed increased nitrous oxide production; sulfide changed both where denitrification occurs (planktonic versus biofilm) and the taxa responsible for denitrification, which resulted in higher abundances of intermediates.

Sulfide increased potential for dissimilatory nitrite reduction to ammonia

We also measured ammonium production during nitrite and nitrate fed conditions and found DNRA occurred during these experiments. Significant and rapid ammonium production occurred during batch experiments with sulfide and $^{15}NO_2^-$ (Fig. 5). However, due to the consumption of ammonium during the experiment, we could not reliably
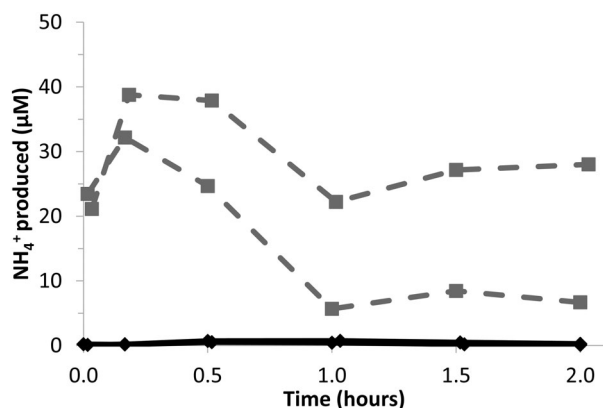
Fig 5. Labelled ammonium profile in experiment with labelled nitrite fed (experiment C), with and without sulfide present in the influent. Dashed grey lines are sulfide amended; solid black lines are experiments without sulfide.

calculate a DNRA rate. Nevertheless, this result indicates that DNRA has the potential to be an important process in this system when sulfide was in the influent. During experiments with $^{15}NO_3^-$ in the influent there was little measurable ammonium produced (<0.5 μM), irrespective of the presence of sulfide. This can likely be explained by the large nitrite pool in these experiments, thereby any $^{15}NO_3^-$ that was reduced to $^{15}NO_2^-$ was diluted by a large pool of $^{14}NO_2^-$, and the probability of the ^{15}N being reduced further to ammonium was relatively small. Therefore, the lack of ammonium production in the experiments with $^{15}NO_3^-$ does not necessarily exclude the potential for DNRA with nitrate as the electron acceptor. In addition to the change in ammonium production observed in the rate experiments, over the long-term stepwise increases in sulfide, the relative abundance of nitrite reductase genes responsible for DNRA (*nrfA* and *nirB/nirD*) increased with increasing sulfide (Fig. 4 and Supplementary Information, Fig. S5). The potential increase in the importance of DNRA within the MABR is also supported by the data from the long-term operation in which ammonium concentrations were shown to increase over time and with sulfide addition (Fig. S3).

Sulfide has been shown to increase DNRA in both natural (Brunet and Garcia-Gil, 1996; Jones *et al*., 2017; Murphy *et al*., 2020) and engineered systems (Dolejs *et al*., 2014; Yin *et al*., 2015). As discussed earlier, sulfide acts as a reducing agent, and electron-rich environments are more prone to DNRA (van den Berg *et al*., 2015). In studies published to date, it is unclear whether the organisms responsible for DNRA use sulfide as an electron donor. In this study, the influent did not have organic compounds that are typically thought to be involved in DNRA (e.g. acetate). The only other electron donor that was present in the reactor was methane. Metatranscriptomic studies have shown methane could be an electron donor for

DNRA in archaeal denitrifying anaerobic methane oxidizers (Arshad *et al*., 2015). Ca. *Methylomirabilis oxyfera* was the more abundant denitrifying anaerobic methane oxidizer in this system and is not known to perform DNRA, though the genetic potential was present via *nirB/nirD*. Based on the data available and current knowledge on DNRA, sulfide is the most likely electron donor for DNRA during these experiments.

We identified MAGs that had DNRA genes and found *nrfA* was present mainly in organisms in the *Anaerolineaceae* family in the planktonic phase that has dissimilatory sulfide potential (*sqr* and *sat*) or in anammox bacteria (*Ca*. Brocadiaceae) in the biofilm (Fig. 4). DNRA by anammox bacteria is known to occur (Kartal *et al*., 2007), but so far has been limited to the use of volatile fatty acids as electron donors, which were not present in the reactor feed. Interestingly, unlike conventional DNRA, low carbon:nitrogen ratios have been shown to induce DNRA by anammox (Castro-Barros *et al*., 2017). However, it is still unlikely that volatile fatty acids that are typically used by anammox were formed in the reactor in sufficient quantities to support anammox growth via DNRA. Thus, we infer that the increased abundances of anammox-associated DNRA genes were likely a byproduct of anammox growth. *nirB* was most abundant in the methane-oxidizing organisms (*Ca*. Methylomirabilis and Methylococcaceae), but DNRA with methane has not been confirmed. Therefore, the observed DNRA was most likely due to sulfide-oxidizing nitrate/nitrate reducers in the planktonic phase, though we cannot rule out contributions from the hypothetical metabolisms inferred here from metagenomic data.

From a treatment standpoint, the goal of biological wastewater treatment processes is to reduce nitrite to nitrogen gas instead of ammonia. Previous literature in both pure cultures and mixed wastewater systems found that at higher sulfide:nitrogen (S:N) ratio, nitrate is reduced to ammonia, while at lower S:N ratios denitrification occurs (Dolejs *et al*., 2014; Yin *et al*., 2015). The ratio of S:N that induced DNRA in these studies ranged from 0.7 to 1.3 mol S/mol N. In our rate experiments, the initial measured S:N ratio was significantly lower than this (0.07–0.12 mol S/mol N). As mentioned previously, this is an underestimate as oxidation likely occurred during reactor filling. The expected S/N ratio based on how much sulfide was added, instead of how much was measured in the first time point, is 0.6 mol S/mol N which is still lower than the ranges that were previously measured. On the other hand, it is possible that the concentration of sulfide, not the S:N ratio, controls DNRA, as has been shown in pure culture studies of DNRA using carbon (Vuono *et al*., 2018). Future work should assess the operating conditions, S:N ratios and concentrations of sulfide that would limit DNRA and induce denitrification, which is preferential for meeting

wastewater treatment goals. Our results underscore the importance of considering DNRA when describing sulfur–nitrogen interactions and their effect on overall community function and reactor performance.

We have shown the potential functions and microbial interactions that result from increases in sulfide in a bio-reactor containing both planktonic and biofilm environments (Fig. 6). Nitrite oxidation was inhibited by sulfide at the highest concentration tested, whereas we observed slight increases in rates of ammonia oxidation in the presence of sulfide. Through both metagenomic and experimental rate data we showed sulfide also led to increased dissimilatory reduction of nitrite to ammonia. We also observed an increase in nitrous oxide production as a result of sulfide addition. In summary, sulfide changed microbial cross-feeding relationships. Due to the tight interactions within the community, it was only through the application of metagenomics and isotopic rate experiments that we could uncover these relationships. In practice, these results can inform the design of engineered treatment systems targeting nitrogen removal. The results also show that it is important to understand how to encourage denitrification over DNRA, especially as there is growing interest in harnessing sulfide as an electron donor for denitrification.

Experimental procedures

Reactor design and inoculation

The MABR system (1.93 L working volume, SI 1, Fig. S1) was modelled after Gilmore *et al.* (2013), inspired by systems operated by a research team at the NASA Kennedy Space Centre (Tansel *et al.*, 2005). Synthetic wastewater was recirculated parallel to the membranes at flow rates greater than 50 times the influent flow rate. DO, ORP, pH, ammonia, and nitrate sensors (YSI/Xylem, Yellow Springs, Ohio, USA) were used to continuously monitor performance. Data were logged using a data acquisition device (NI 6008) and Labview program (National Instruments, Austin, Texas, USA). The program was also used to control pH (by controlling a pump feeding a 30 g/L sodium bicarbonate solution) and air addition (by controlling a mass flow controller connected to a pressurized air cylinder (GFCS17A, Aalborg, Aalborg, Denmark)). Details of reactor startup conditions and inocula are provided in the Supporting Information Section 1. Briefly, the reactor was inoculated with a mixture of a previously established community (Delgado Vela *et al.*, 2015a) and activated sludge from an Anaerobic–Anoxic–Aerobic activated sludge process (Ann Arbor, MI).
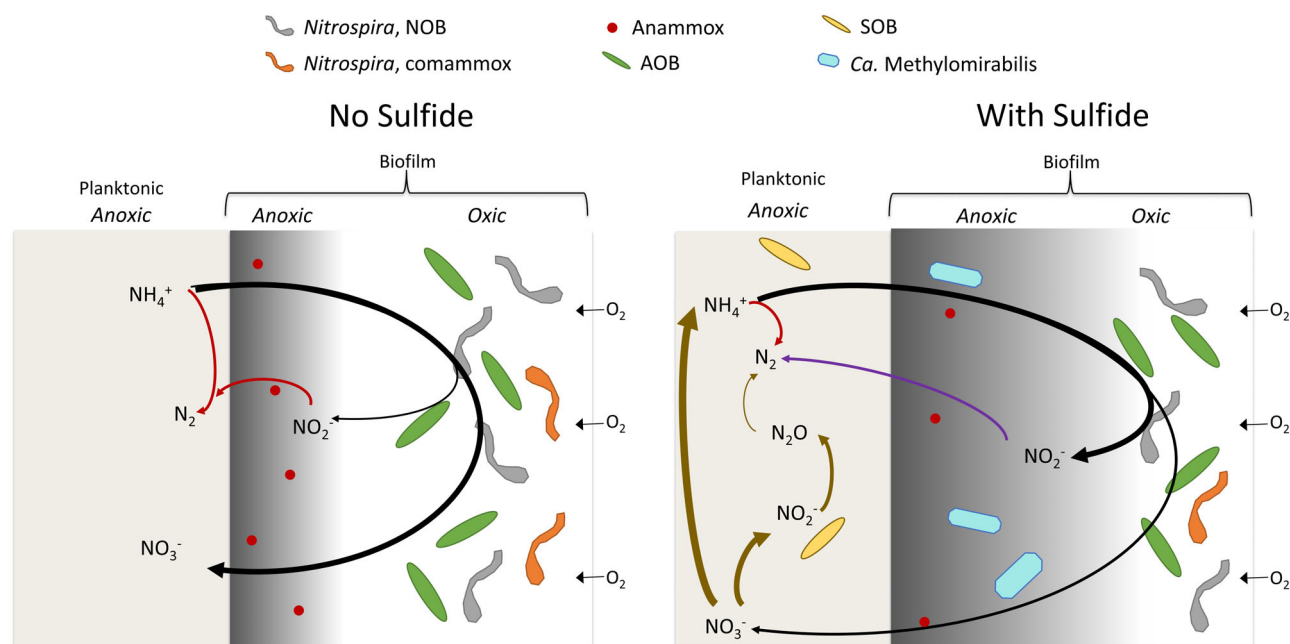

Fig 6. Potential nitrogen metabolisms with and without sulfide that resulted from long-term increases in sulfide. Sulfide shifts redox in the biofilm as indicated by a shift in greyscale. Arrow colour indicates metabolism responsible: black is nitrifying bacteria; purple denitrification linked to either anammox or anaerobic methane oxidation (Ca. Methylomirabilis); red is anammox; brown is DNRA and denitrification by sulfide oxidizing bacteria (SOB). Coloured arrows also indicate electron donor: purple is either methane or ammonia, red is ammonia, and brown is sulfide. Arrow thickness indicates the relative rate at which different processes occur.

Reactor influent and operation

The reactor was operated to simulate treatment of an effluent from a mainstream anaerobic process. Synthetic influent (20 L) was prepared as described elsewhere (Bekele *et al*., 2020) and in the Supporting Information. The synthetic influent was prepared approximately every 2 days using glassware that was autoclaved prior to influent preparation. The influent contained ammonium at a concentration of 30 mg/L as N and was saturated with methane. For the first 120 days of operation (Phase A), a nitrifying biofilm was established with steady increases in influent ammonium loading (Table S1 and Fig. S2). After this initial period, phase B was begun with stepwise increases in the sulfide concentration over the course of 299 days (Table S1, Figs 1 and S3). To minimize precipitation, sodium sulfide was added via a separate peristaltic pump to achieve the desired influent concentration. The sulfide feed was made using a sodium sulfide non-ahydrate stock (5 g/L as sulfur) stored in an anaerobic chamber. The feed jar with sodium sulfide was connected to a gas bag with nitrogen gas to prevent aerobic oxidation. After sulfide was added, a planktonic phase grew and became abundant. As the original purpose of the study was to support a biofilm phase, the planktonic phase was regularly cleaned by cleaning all the tubing and the flow cells approximately once per month. This planktonic phase was included in biomass samples (described below).

Bulk reactor rate experiments

Process rate determinations were carried out in three batch experiments (each receiving a different ^{15}N labelled substrate (>98% purity, Sigma Aldrich)), which were conducted in duplicate with and without sulfide in the influent (12 experiments total, summarized in Supplementary Information Table S3). Initial rates of reaction were obtained during the batch experiments and, consequently, represent potential rates. In addition, before each set of bulk reactor rate experiments the flow cells and planktonic phase were cleaned. The benefit of conducting the experiments in this manner is that multiple substrate profiles could be assessed in replicate experiments.

To conduct rate experiments, the reactor was emptied, refilled with influent containing a ^{15}N substrate and operated in batch mode with recirculation but no new influent for 2 h. To obtain rates of ammonia oxidation, ^{15}N-NH$_4^+$ and ^{14}N-NO$_2$ (Experiment A) were added to the influent and the production of ^{15}NO$_2^-$ + ^{15}NO$_3^-$ was measured, $^{45 + 46}$N$_2$O was also measured to look for N$_2$O production. Experiment B was used to obtain rates of nitrate reduction and N$_2$O production with ^{15}N-NO$_3^-$, ^{14}N-NO$_2^-$,

and ^{14}N-NH$_4^+$ added to the influent and measuring the production of ^{15}NO$_2^-$ and $^{45 + 46}$N$_2$O. In experiment C the influent contained ^{15}N-NO$_2^-$ and ^{14}N-NO$_3^-$ to obtain rates of nitrite oxidation (^{15}NO$_3^-$ production) and DNRA (^{15}NH$_4^+$ production). All amendments, both ^{15}N and ^{14}N pools, are shown in Supplementary Information Table S3. To initiate an experiment, the reactor was filled with new influent, which took between 15 and 20 min. The reactor was sampled immediately after the recirculation pump was turned on (time zero) and 10, 30, 60, 90, and 120 min thereafter. It is likely that sulfide oxidation started before mixing (via the recirculation pump) could begin. However, this potential activity is not included in the rate measurements, as the time zero sample was taken as mixing commenced. This sampling scheme was chosen to keep our rate determinations conservative. The time between the experiments was at a minimum equivalent to four hydraulic residence times (HRT = 5.1 h) to minimize the residual label in the bioreactor. To correct for any residual label from the previous experiment, the reactor was also sampled approximately 30 min before the experiment and a few hours after the experiment was over. The labelled substrate measured in the before samples were below 0.7% of the influent label for all experiments. All the experiments with sulfide were conducted first, between days 547 and 552. Sulfide was removed from the influent long enough for effluent nitrogen to mimic previous sulfide-free operation (2 days), then experiments without sulfide were conducted on days 557–562.

At each time point, a 15 ml sample was collected and filtered (0.2 μm PES, Titan3™, Thermo Fisher Scientific) and measured for pH, before being stored frozen. Additionally, a sample was taken for N$_2$O analysis in a 12 ml exetainer (LabCo, UK), which contained a glass bead, filled with overflow and 100 μl of 50% wt./vol. ZnCl$_2$ was added, then capped bubble-free, shaken and stored at room temperature until analysis. To avoid introducing air into the recirculation line, the liquid taken for each sample was replenished with either sodium bicarbonate or distilled water (depending on if any pH adjustment was needed). Standard protocols were used to measure nitrite, nitrate and ammonium (Grasshoff, 2009; Garcia-Robledo, 2014). Process rates were determined from ^{15}N increase over time, using methods previously described by Bristow *et al*., (2016). Briefly, for analysis of ^{15}NO$_3^-$, residual ^{15}NO$_2^-$ was first removed from the sample using sulfamic acid (Füssel *et al*., 2012), followed by cadmium reduction to convert ^{15}NO$_3^-$ to ^{15}NO$_2^-$ and sulfamic acid to reduce the ^{15}NO$_2^-$ to N$_2$ (McIlvin and Altabet, 2005). For nitrate reduction rates the ^{15}NO$_2^-$ produced was converted to N$_2$ with sulfamic acid (Füssel *et al*., 2012). For the determination of ^{15}NH$_4^+$ production, NH$_4^+$ was converted to N$_2$ using hypobromite (Warembourg, 1993).

All of these preparation procedures produce N_2 ($^{14}N^{15}N$ and $^{15}N^{15}N$) which was analysed using a gas chromatography-isotope ratio mass spectrometer (GC-IRMS), as described in Dalsgaard *et al.*, (2012). N_2O production from $^{15}NH_4^+$ and $^{15}NO_3^-$ additions was measured on a GC-IRMS, customized TraceGas coupled to a multicollector IsoPrime 100 at the Max Planck Institute for Microbiology, Bremen, Germany. We were unable to quantify ^{15}N-N_2O production after $^{15}NO_2^-$ addition due to technical issues arising from side reactions caused by the combination of $ZnCl_2$ and H_2S. Each time point was individually corrected for ^{15}N labeling percentage and all rates were inferred from the slopes of linear regression across the first hour of the experiment to minimize potential interactions with consumption processes ($R^2 > 0.93$ for all rates).

For experiments with sulfide in the influent, samples for sulfide analysis were collected separately, immediately after the samples for process rates. Samples were collected, stored and analysed according to method 4500-S^{2-} G in Standard Methods (APHA *et al.*, 2005). Sulfide samples were diluted ($2\times$) in sulfide antioxidant buffer. They were immediately transferred to the anaerobic chamber, filtered (0.45 μm, nitrocellulose filter, Fisher Scientific) and preserved in the dark. All samples were analysed within 24 h. Sulfide was analysed using a silver sulfide electrode (Thermo Scientific, Orion) that was calibrated by making standards with a 3% (wt./vol.) sodium sulfide stock solution (Ricca Chemical Company), according to method 4500-S^{2-} G (APHA *et al.*, 2005) with a limit of detection of 0.3 μM.

Biomass sampling, DNA extraction, qPCR and metagenomic sequencing

Biofilm samples were collected by opening the top flange of the reactor and carefully scraping the lumen of the membrane. When there was sufficient planktonic growth, biomass samples from the monitoring probe flow cells were also collected. Duplicate biomass samples collected during reactor operation on days 117, 249, 368, and 479 were submitted for sequencing. In addition, samples were sequenced from when the reactor was decommissioned (day 565). Duplicate samples taken from the outer membranes at a midpoint vertical height and from biomass that had settled at the bottom of the reactor chamber were submitted for sequencing (referred to as sloughed). DNA extractions were performed by combining bead beating with the Maxwell automatic DNA extractor as previously described (Delgado Vela *et al.*, 2018).

Gene copies of bacterial ammonia monooxygenase (*amoA*), 16S rRNA, *Nitrospira* nitrite oxidoreductase genes (*nxrB*), anammox 16S genes, and comammox clade A *amoA* genes were quantified in triplicate using qPCR. Purified products from PCR reactions on reactor samples were used as standards for the qPCR reaction. For all qPCR targets except the 16S rRNA gene, standards were confirmed using Sanger Sequencing. Positive controls (DNA extracts from a nitrifying enrichment culture for AOB and *Nitrospira* (Stadler and Love, 2016), DEMON sludge for anammox, drinking water biofilter for comammox (Pinto *et al.*, 2015), or genomic DNA from a *Pseudomonas aeruginosa* pure culture for 16S) and duplicate no-template controls were analysed on each qPCR plate. Details on qPCR conditions and primers are given in the Supporting Information Section 3.

Samples were submitted for shotgun sequencing on the Illumina HiSeq 4000 platform with 150 base pair paired-end reads with a target insert size of 350 base pairs at the University of Michigan DNA Sequencing Core. DNA was fragmented using standard Covaris sonication (Covaris, Woburn, MA). Fragmented DNA was then prepared as a standard Illumina library using Wafergen reagents on the Apollo 324™ instrument, where the fragments are end-repaired, A tailed, and adapter-ligated. Then, the samples are PCR amplified and pooled for sequencing. Final libraries were checked for quality and quantity by TapeStation (Agilent, Santa Clara, CA) and qPCR using Roche's library quantification kit for Illumina Sequencing platforms (catalogue # KK4835). They were clustered on the cBot (Illumina) and were pooled and sequenced on a 300 cycle paired end run on a HiSeq 4000 using software version 3.4.0.38.

Whole-genome assembly and annotation

Raw sequencing reads were dereplicated (100% identity over 100% of the length for both forward and reverse reads), trimmed using Sickle (Joshi and Fass, 2011), and adaptors were removed using bbduk (Bushnell, 2014). Trimming removed 5 ± 1% of the data. Trimmed metagenomic reads are available on the NCBI Sequence Read Archive database, accession number PRJNA598204. Whole-genome *de novo* assembly was performed on pooled duplicate samples using MEGAHIT v 1.1.2 (Li *et al.*, 2015) with mink = 27, maxk = 141 and a step size of 10. Assembled data resulted in 390 000 ± 78 000 contigs (of which 150 000 ± 29 000 contigs were >1000 bp). The N50 of the assembled contigs was 4000 ± 480 bp. Reads were mapped to assembled contigs using the Burrows-Wheeler Aligner (BWA version 0.7.15) and default parameters (Li and Durbin, 2009). The mapped read counts were extracted using SAMtools version 1.3.1 (Li *et al.*, 2009). Each duplicate sample was mapped to the pooled assembly separately. Gene calling on assembled data was performed using Prodigal v2.6.2. The predicted amino acid

sequences were then compared with a custom database of relevant functions (Supplementary Information - Table S7) using BLASTp. The database was generated using relevant functions from whole genomes of taxa represented in previously analysed 16S rRNA gene amplicon sequencing data. The outputs were filtered based on an alignment length of at least 100 amino acids, bitscores above 250, and percent identities greater than 50%. Gene annotation was confirmed by manually checking the annotations against the entire NCBI non-redundant database for each hit. Assembled contigs were submitted to the DOE JGI-IMG/MER annotation pipeline (GOLD Study ID Gs0134229). KEGG annotations obtained from IMG for the functions that are in the custom databases were downloaded, confirmed manually via BLAST against the entire NCBI non-redundant database, and incorporated into the final annotations. To determine relative abundances of genes, coverages were normalized to the coverage of the *recA* gene in the whole community (annotations from IMG) and the length of the genes.

Metagenomic binning and analysis

The annotation and BLAST analysis revealed that coverages of important organisms were likely high (greater than 200× coverage). To improve the assembly and binning on important organisms, trimmed reads were subsampled, and reassembled as previously described (Hug *et al*., 2016). Reads were subsampled to 20% to achieve this goal. Assemblies and mapping of downsampled reads were performed using the same methods as the complete samples. CONCOCT v0.4.1 was used to bin assembled reads (both complete assemblies and downsampled assemblies) using default parameters. Bin completeness and contamination were evaluated using CheckM v1.0.11. dRep was used to find unique bins across all samples (bins resulting from complete and downsampled assemblies) (Olm *et al*., 2017). Dereplicated bins that were greater than 90% complete, had less than 10% contamination, and had a functional gene hit from the custom database were taxonomically identified using PhyloSift. Any bins with a clean taxonomic assignment determined using PhyloSift (defined as greater than 90% of the contigs were the same Family) were considered high-quality bins. We obtained 44 bins that met these criteria.Details of these bins are provided in Table S8 in supplementary data and have been uploaded to IMG (accession numbers available in Supporting Information). To obtain relative abundances of the bins, QC'd reads were mapped back to a fasta file containing all 44 high-quality bins obtained from the analysis. The relative abundance of the bin was calculated by taking the average coverage across the bin and normalizing the coverage to the summation of all *recA* coverage from the sample.

Statistical analysis

Associations between gene coverages, bin coverages, and sulfide concentration were tested using repeated measures ANOVA and corrected for multiple comparisons using the Benjamini-Hochberg correction factor. Differences in rate measurements were tested using a two-sided *t*-test. The R environment was used to analyse all data (R Core Team, 2016).

References

APHA, AWWA, and WEF. (2005) *Standard Methods for the Examination of Water and Wastewater*, 21st ed. Washington, DC: American Public Health Association.

Arshad, A., Martins, P.D., Frank, J., Jetten, M.S.M., Op den Camp, H.J.M., and Welte, C.U. (2017) Mimicking microbial interactions under nitrate-reducing conditions in an anoxic bioreactor: enrichment of novel Nitrospirae bacteria distantly related to Thermodesulfovibrio. *Environ Microbiol* **19**: 4965–4977.

Arshad, A., Speth, D.R., de Graaf, R.M., Op den Camp, H.J. M., Jetten, M.S.M., and Welte, C.U. (2015) A metagenomics-based metabolic model of nitrate-dependent anaerobic oxidation of methane by methanoperedens-like archaea. *Front Microbiol* **6**: 1–14.

Beck, D.A.C., Kalyuzhnaya, M.G., Malfatti, S., Tringe, S.G., Glavina del Rio, T., Ivanova, N., *et al*. (2013) A metagenomic insight into freshwater methane-utilizing communities and evidence for cooperation between the Methylococcaceae and the Methylophilaceae. *PeerJ* **2013**: 1–23.

Bejarano-Ortiz, D.I., Huerta-Ochoa, S., Thalasso, F., Cuervo-López, F.d.M., and Texier, A.-C. (2015) Kinetic constants for biological ammonium and nitrite oxidation processes under sulfide inhibition. *Appl Biochem Biotechnol* **177**: 1665–1675.

Bekele, Z.A., Delgado Vela, J., Bott, C.B., and Love, N.G. (2020) Sensor-mediated granular sludge reactor for

nitrogen removal and reduced aeration demand using a dilute wastewater. *Water Environ Res* **92**: 1006–1016.

Bristow, L.A., Dalsgaard, T., Tiano, L., Mills, D.B., Bertagnolli, A.D., Wright, J.J., *et al*. (2016) Ammonium and nitrite oxidation at nanomolar oxygen concentrations in oxygen minimum zone waters. *Proc Natl Acad Sci U S A* **113**: 10601–10606.

Brunet, R.C., and Garcia-Gil, L.J. (1996) Sulfide-induced dissimilatory nitrate reduction to ammonia in anaerobic freshwater sediments. *FEMS Microbiol Ecol* **21**: 131–138.

Bushnell, B. (2014) *BBTools software package*. http://sourceforgenet/projects/bbmap.

Canfield, D.E., Stewart, F.J., Thamdrup, B., De Brabandere, L., Delong, E.F., Revsbech, N.P., and Ulloa, O. (2010) A cryptic sulfur cycle in oxygen-minimum-zone waters off the Chilean coast. *Science* **330**: 1375–1378.

Castro-Barros, C.M., Jia, M., van Loosdrecht, M.C.M., Volcke, E.I.P., and Winkler, M.K.H. (2017) Evaluating the potential for dissimilatory nitrate reduction by anammox bacteria for municipal wastewater treatment. *Bioresour Technol* **233**: 363–372.

D'Souza, G., Shitut, S., Preussger, D., Yousif, G., Waschina, S., and Kost, C. (2018) Ecology and evolution of metabolic cross-feeding interactions in bacteria. *Nat Prod Rep* **35**: 455–488.

Daims, H., Lebedeva, E.V., Pjevac, P., Han, P., Herbold, C., Albertsen, M., *et al*. (2015) Complete nitrification by Nitrospira bacteria. *Nature* **528**: 504–509.

Dalsgaard, T., Thamdrup, B., Farías, L., and Revsbech, N.P. (2012) Anammox and denitrification in the oxygen minimum zone of the eastern South Pacific. *Limnol Oceanogr* **57**: 1331–1346.

Delgado Vela, J., Dick, G.J., and Love, N.G. (2018) Sulfide inhibition of nitrite oxidation in activated sludge depends on microbial community composition. *Water Res* **138**: 241–249.

Delgado Vela, J., Martin, K.J., Beaton, N., McFarland, A., Stadler, L.B., Bott, C.B., *et al*. (2015a) Nutrient removal from mainstream anaerobic processes using a membrane biofilm reactor and a granular sludge sequencing batch reactor. In *Proceedings of the Water Environment Federation*.

Delgado Vela, J., Stadler, L.B., Martin, K.J., Raskin, L., Bott, C.B., and Love, N.G. (2015b) Prospects for biological nitrogen removal from anaerobic effluents during mainstream wastewater treatment. *Environ Sci Technol Lett* **2**: 233–244.

Dolejs, P., Paclík, L., Maca, J., Pokorna, D., Zabranska, J., and Bartacek, J. (2014) Effect of S/N ratio on sulfide removal by autotrophic denitrification. *Appl Microbiol Biotechnol* **99**: 2383–2392.

Downing, L.S., and Nerenberg, R. (2008) Total nitrogen removal in a hybrid, membrane-aerated activated sludge process. *Water Res* **42**: 3697–3708.

Erguder, T.H., Boon, N., Vlaeminck, S.E., and Verstraete, W. (2008) Partial nitrification achieved by pulse sulfide doses in a sequential batch reactor. *Environ Sci Technol* **42**: 8715–8720.

Ettwig, K.F., Butler, M.K., Le Paslier, D., Pelletier, E., Mangenot, S., Kuypers, M.M.M., *et al*. (2010) Nitrite-driven anaerobic methane oxidation by oxygenic bacteria. *Nature* **464**: 543–548.

Füssel, J., Lam, P., Lavik, G., Jensen, M.M., Holtappels, M., Günter, M., and Kuypers, M.M.M. (2012) Nitrite oxidation in the Namibian oxygen minimum zone. *ISME J* **6**: 1200–1209.

Füssel, J., Lücker, S., Yilmaz, P., Nowka, B., van Kessel, M. A.H.J., Bourceau, P., *et al*. (2017) Adaptability as the key to success for the ubiquitous marine nitrite oxidizer Nitrococcus. *Sci Adv* **3**: e1700807.

García-Robledo, E., Corzo, A., and Papaspyrou, S. (2014). A fast and direct spectrophotometric method for the sequential determination of nitrate and nitrite at low concentrations in small volumes. *Mar Chem*, **162**, 30–36.

Grasshoff, K., Kremling, K., & Ehrhardt, M. (2009). Methods of seawater analysis. Hoboken, NJ: John Wiley & Sons.

Gilmore, K.R., Terada, A., Smets, B.F., Love, N.G., and Garland, J.L. (2013) Autotrophic nitrogen removal in a membrane-aerated biofilm reactor under continuous aeration: a demonstration. *Environ Eng Sci* **30**: 38–45.

Guerrero-Cruz, S., Cremers, G., van Alen, T.A., Op den Camp, H.J.M., Jetten, M.S.M., Rasigraf, O., and Vaksmaa, A. (2018) Response of the anaerobic methanotroph "Candidatus Methanoperedens nitroreducens" to oxygen stress. *Appl Environ Microbiol* **84**: 1–17.

Heffernan, B., Shrivastava, A., Toniolo, D., Semmens, M., and Syron, E. (2017) Operation of a large scale membrane aerated biofilm reactor for the treatment of municipal wastewater. *Proc Water Environ Fed* **2017**: 285–297.

Houweling, D., Peeters, J., Cote, P., Long, Z., and Adams, N. (2017) Proving membrane aerated biofilm reactor (MABR) performance and reliability: results from four pilots and a full-scale plant. *Proc Water Environ Fed* **2017**: 272–284.

Hug, L.A., Thomas, B.C., Sharon, I., Brown, C.T., Sharma, R., Hettich, R.L., *et al*. (2016) Critical biogeochemical functions in the subsurface are associated with bacteria from new phyla and little studied lineages. *Environ Microbiol* **18**: 159–173.

Jin, R.-C., Yang, G.-F., Zhang, Q.-Q., Ma, C., Yu, J.-J., and Xing, B.-S. (2013) The effect of sulfide inhibition on the ANAMMOX process. *Water Res* **47**: 1459–1469.

Jones, Z.L., Jasper, J.T., Sedlak, D.L., and Sharp, J.O. (2017) Sulfide induced dissimilatory nitrate reduction to ammonium supports anaerobic ammonium oxidation (Anammox) in an open-water unit process wetland. *Appl Environ Microbiol* **83**: 1–14.

Joshi, N.A. and Fass, J.N. (2011) Sickle: A sliding-window, adaptive, quality-based trimming tool for FastQ files (Version 1.33). https://github.com/najoshi/sickle

Joye, S.B., and Hollibaugh, J.T. (1995) Influence of sulfide inhibition of nitrification on nitrogen regeneration in sediments. *Science* **270**: 623–625.

Kartal, B., Kuypers, M.M.M., Lavik, G., Schalk, J., Op den Camp, H.J.M., Jetten, M.S.M., *et al*. (2007) Anammox bacteria disguised as denitrifiers: nitrate reduction to dinitrogen gas via nitrite and ammonium. *Environ Microbiol* **9**: 635–642.

Koch, H., Lücker, S., Albertsen, M., Kitzinger, K., Herbold, C., Spieck, E., *et al*. (2015) Expanded metabolic versatility of ubiquitous nitrite-oxidizing bacteria from the

genus Nitrospira. *Proc Natl Acad Sci U S A* **112**: 11371–11376.

Kuypers, M.M.M., Marchant, H.K., and Kartal, B. (2018) The microbial nitrogen-cycling network. *Nat Rev Microbiol* **16**: 263–276.

Li, D., Liu, C.-M., Luo, R., Sadakane, K., and Lam, T.-W. (2015) MEGAHIT: an ultra-fast single-node solution for large and complex metagenomics assembly via succinct de Bruijn graph. *Bioinformatics* **31**: 1674–1676.

Li, H., and Durbin, R. (2009) Fast and accurate short read alignment with Burrows-Wheeler transform. *Bioinformatics* **25**: 1754–1760.

Li, H., Handsaker, B., Wysoker, A., Fennell, T., Ruan, J., Homer, N., *et al*. (2009) The sequence alignment/map format and SAMtools. *Bioinformatics* **25**: 2078–2079.

Liu, J., Sun, F., Wang, L., Ju, X., Wu, W., and Chen, Y. (2014) Molecular characterization of a microbial consortium involved in methane oxidation coupled to denitrification under micro-aerobic conditions. *J Microbial Biotechnol* **7**: 64–76.

Lucker, S., Wagner, M., Maixner, F., Pelletier, E., Koch, H., Vacherie, B., *et al*. (2010) A Nitrospira metagenome illuminates the physiology and evolution of globally important nitrite-oxidizing bacteria. *Proc Natl Acad Sci U S A* **107**: 13479–13484.

Luebke, J.L., Shen, J., Bruce, K.E., Kehl-Fie, T.E., Peng, H., Skaar, E.P., and Giedroc, D.P. (2014) The CsoR-like sulfurtransferase repressor (CstR) is a persulfide sensor in *Staphylococcus aureus*. *Mol Microbiol* **94**: 1343–1360.

Lüke, C., Speth, D.R., Kox, M.A.R., Villanueva, L., and Jetten, M.S.M. (2016) Metagenomic analysis of nitrogen and methane cycling in the Arabian Sea oxygen minimum zone. *PeerJ* **4**: e1924.

Manconi, I., van der Maas, P., and Lens, P. (2006) Effect of copper dosing on sulfide inhibited reduction of nitric and nitrous oxide. *Nitric Oxide - Biol Chem* **15**: 400–407.

Marchant, H.K., Tegetmeyer, H.E., Ahmerkamp, S., Holtappels, M., Lavik, G., Graf, J., *et al* (2018) Metabolic specialization of denitrifiers in permeable sediments controls N_2O emissions. *Environ Microbiol* **20**: 4486–4502.

Martin, K.J., and Nerenberg, R. (2012) The membrane biofilm reactor (MBfR) for water and wastewater treatment: principles, applications, and recent developments. *Bioresour Technol* **122**: 83–94.

McIlvin, M.R., and Altabet, M.A. (2005) Chemical conversion of nitrate and nitrite to nitrous oxide for nitrogen and oxygen isotopic analysis in freshwater and seawater. *Anal Chem* **77**: 5589–5595.

Modin, O., Fukushi, K., and Yamamoto, K. (2007) Denitrification with methane as external carbon source. *Water Res* **41**: 2726–2738.

Morgenroth, E., Sherden, T., Van Loosdrecht, M.C.M., Heijnen, J.J., and Wilderer, P.A. (1997) Aerobic granular sludge in a sequencing batch reactor. *Water Res* **31**: 3191–3194.

Murphy, A.E., Bulseco, A.N., Ackerman, R., Vineis, J.H., and Bowen, J.L. (2020) Sulphide addition favours respiratory ammonification (DNRA) over complete denitrification and alters the active microbial community in salt marsh sediments. *Environ Microbiol* **22**: 2124–2139.

Olm, M.R., Brown, C.T., Brooks, B., and Banfield, J.F. (2017) DRep: a tool for fast and accurate genomic comparisons that enables improved genome recovery from metagenomes through de-replication. *ISME J* **11**: 2864–2868.

Osaka, T., Ebie, Y., Tsuneda, S., and Inamori, Y. (2008) Identification of the bacterial community involved in methane-dependent denitrification in activated sludge using DNA stable-isotope probing. *FEMS Microbiol Ecol* **64**: 494–506.

Peeters, J., Long, Z., Houweling, D., Côté, P., Daigger, G.T., and Snowling, S. (2017) Nutrient removal intensification with MABR–developing a process model supported by piloting. *Proc Water Environ Fed* **2017**: 657–669.

Pinto, A.J., Marcus, D.N., Ijaz, Z., Bautista-de los Santos, Q. M., Dick, G.J., and Raskin, L. (2015) Metagenomic evidence for the presence of Comammox Nitrospira-like bacteria in a drinking water system. *mSphere* **1**: e00054-15.

Pochana, K., and Keller, J. (1999) Study of factors affecting simultaneous nitrification and denitrification (SND). *Water Sci Technol* **39**: 61–68.

R Core Team. (2016) R: A Language and Environment for Statistical Computing.

Reim, A., Lüke, C., Krause, S., Pratscher, J., and Frenzel, P. (2012) One millimetre makes the difference: high-resolution analysis of methane-oxidizing bacteria and their specific activity at the oxic-anoxic interface in a flooded paddy soil. *ISME J* **6**: 2128–2139.

Rios-Del Toro, E.E., and Cervantes, F.J. (2016) Coupling between anammox and autotrophic denitrification for simultaneous removal of ammonium and sulfide by enriched marine sediments. *Biodegradation* **27**: 107–118.

Russ, L., Speth, D.R., Jetten, M.S.M., Op den Camp, H.J.M. M., and Kartal, B. (2014) Interactions between anaerobic ammonium and sulfur-oxidizing bacteria in a laboratory scale model system. *Environ Microbiol* **16**: 3487–3498.

Russ, L., van Alen, T.A., Jetten, M.S.M., Op den Camp, H.J. M., and Kartal, B. (2019) Interactions of anaerobic ammonium oxidizers and sulfide-oxidizing bacteria in a substrate-limited model system mimicking the marine environment. *FEMS Microbiol Ecol* **95**: fiz137.

Senga, Y., Mochida, K., Fukumori, R., Okamoto, N., and Seike, Y. (2006) N_2O accumulation in estuarine and coastal sediments: the influence of H_2S on dissimilatory nitrate reduction. *Estuar Coast Shelf Sci* **67**: 231–238.

Seth, E.C., and Taga, M.E. (2014) Nutrient cross-feeding in the microbial world. *Front Microbiol* **5**: 1–6.

Sorensen, J., Tiedje, J.M., and Firestone, R.B. (1980) Inhibition by sulfide of nitric and nitrous-oxide reduction by denitrifying Pseudomonas-Fluorescens. *Appl Environ Microbiol* **39**: 105–108.

Stadler, L.B., and Love, N.G. (2016) Impact of microbial physiology and microbial community structure on pharmaceutical fate driven by dissolved oxygen concentration in nitrifying bioreactors. *Water Res* **104**: 189–199.

Tansel, B., Sager, J., Rector, T., Garland, J., Strayer, R.F., Levine, L., *et al*. (2005) Integrated evaluation of a sequential membrane filtration system for recovery of bioreactor effluent during long space missions. *J Membr Sci* **255**: 117–124.

Terada, A., Lackner, S., Tsuneda, S., and Smets, B.F. (2007) Redox-stratification controlled biofilm (ReSCoBi) for completely autotrophic nitrogen removal: the effect of co- versus counter-diffusion on reactor performance. *Biotechnol Bioeng* **97**: 40–51.

Thorup, C., and Schramm, A. (2017) Disguised as a sulfate reducer: growth of the Deltaproteobacterium Desulf urivibrio alkaliphilus by sulfide oxidation with nitrate. *MBio* **8**: 1–9.

Tugstas, A.E., and Pavlostathis, S.G. (2007) Effect of sulfide on nitrate reduction in mixed methanogenic cultures. *Biotechnol Bioeng* **97**: 1448–1459.

van de Graaf, A.A., De Bruijn, P., Robertson, L.A., Jetten, M. S.M., and Kuenen, J.G. (1996) Autotrophic growth of anaerobic ammonium-oxidizing micro-organisms in a fluidized bed reactor. *Microbiology* **142**: 2187–2196.

van den Berg, E.M., van Dongen, U., Abbas, B., and Van Loosdrecht, M.C.M. (2015) Enrichment of DNRA bacteria in a continuous culture. *ISME J* **9**: 2153–2161.

van Kessel, M.A.H.J., Speth, D.R., Albertsen, M., Nielsen, P. H., Op den Camp, H.J.M., Kartal, B., *et al*. (2015) Complete nitrification by a single microorganism. *Nature* **528**: 555–559.

Vuono, D.C., Read, R.W., Hemp, J., Sullivan, B.W., Arnone III, J.A., Neveaux, I., *et al*. (2018) Resource limitation modulates the fate of dissimilated nitrogen in dual-pathway Actinobacterium. *bioRxiv*.

Warembourg, F.R. (1993) Nitrogen fixation in soil and plant systems. *Nitrogen Isotopes Techniques* (pp.157–180). New York: Academic Press, Inc.

Xia, Y., Lü, C., Hou, N., Xin, Y., Liu, J., Liu, H., and Xun, L. (2017) Sulfide production and oxidation by heterotrophic bacteria under aerobic conditions. *ISME J* **11**: 2754–2766.

Yin, Z., Xie, L., and Zhou, Q. (2015) Effects of sulfide on the integration of denitrification with anaerobic digestion. *J Biosci Bioeng* **120**: 426–431.

Yu, Z., Beck, D.A.C., and Chistoserdova, L. (2017) Natural selection in synthetic communities highlights the roles of Methylococcaceae and Methylophilaceae and suggests differential roles for alternative methanol dehydrogenases in methane consumption. *Front Microbiol* **8**: 1–13.

Supporting Information

Additional Supporting Information may be found in the online version of this article at the publisher's web-site:

Appendix S1: Supporting information